Stability of synchronous chaos and on-off intermittency in coupled map lattices

Mingzhou Ding* and Weiming Yang†
Program in Complex Systems and Brain Sciences, Center for Complex Systems and Department of Mathematical Sciences, Florida Atlantic University, Boca Raton, Florida 33431
(Received 25 April 1997)

In this paper we consider the stability of synchronous chaos in lattices of coupled N-dimensional maps. For global coupling, we derive explicit conditions for computing the parameter values at which the synchronous chaotic attractor becomes unstable and bifurcates into asynchronous chaos. In particular, we show that after the bifurcation one generally observes on-off intermittency, a process in which the entire system evolves nearly synchronously (but chaotically) for long periods of time, which are interrupted by brief bursts away from synchrony. For nearest-neighbor coupled systems, however, we show that the stability of the synchronous chaotic state is a function of the system size. In particular, for large systems, we will not be able to observe synchronous chaos. We derive a condition relating the local map's largest Lyapunov exponent to the maximal system size under which one can still observe synchronous chaos and on-off intermittency. Other issues related to the characterization of on-off intermittent signals are also discussed. [S1063-651X(97)07210-3]

PACS number(s): 05.40.+j, 05.45.+b

I. INTRODUCTION

Consider a coupled map lattice [1]. Assume that there is a range of parameter values for which this system exhibits a unique attractor of synchronous chaos where every element evolves chaotically and is in synchrony with every other element. Suppose that, as the parameter is varied past a certain bifurcation point, this synchronous chaos loses stability, and is replaced by an asynchronous chaotic state. It can be shown that, under rather general conditions, immediately after the bifurcation, the dynamics exhibits on-off intermittency [3–7] in which long episodes of nearly synchronous evolution (laminar phase) are interrupted by a certain element or elements in the system bursting away from the synchronous state. The bursts become more and more frequent as the parameter is moved further and further away from the bifurcation point. Eventually, the system reaches fully developed heterogeneous chaos where no clearly identifiable episodes of synchronous chaos are seen. According to the terminology of a recent paper [2], this bifurcation is a spatiotemporal example of a nonhysteretic blowout bifurcation. Blowout bifurcations occur in systems with symmetry, which in our case is the spatial translational invariance due to identical elements used at each space site. It is nonhysteretic because there are no other attractors in the phase space coexisting with the synchronous chaos attractor. Hysteretic blowout bifurcations occur if there are simultaneously more than one attractor in the system. In this case one may observe riddled basins on the side of the parameter axis where the synchronous state is still stable [8].

Assume that the local map is N dimensional and is chaotic in the absence of coupling. In Sec. II we carry out a stability analysis of synchronous chaos for globally coupled systems of such maps. We show that, when the synchronous chaos becomes unstable, the system exhibits on-off intermittency. Section III presents numerical results on the characterization of on-off intermittent signals using quantities like laminar phase distribution plots and power spectra. In Sec. VI we consider the stability of synchronous chaos in coupled map lattices where the coupling is nearest neighbor. We point out that, in such systems, we can only expect to see stable synchronous chaos and the accompanying on-off intermittent behavior if the number of coupled maps is small. Section V concludes this paper.

II. STABILITY OF SYNCHRONOUS CHAOS IN GLOBALLY COUPLED MAPS AND ONSET OF ON-OFF INTERMITTENCY

Coupled map lattices, as discrete analogs to coupled oscillators and partial differential equations, have in recent years become the model of choice for developing intuitions and concepts in the study of spatiotemporal dynamical systems [1,9]. Assuming global (mean field) coupling we express our model as

$$\mathbf{x}_{n+1}(i)=(1-\epsilon)\mathbf{f}(\mathbf{x}_n(i))+\frac{\epsilon}{L}\sum_{j=1}^{L}\mathbf{f}(\mathbf{x}_n(j)), \tag{1}$$

where $\mathbf{x}$ is an N-dimensional column vector, n denotes the time step, i,j are labels of lattice sites, $\mathbf{f}(\mathbf{x})$ is an N-dimensional nonlinear mapping function, ϵ is the coupling strength satisfying $0\leqslant\epsilon<1$, and L is the total number of coupled elements. The local N-dimensional map

$$\mathbf{x}_{n+1}=\mathbf{f}(\mathbf{x}_n) \tag{2}$$

is assumed to be chaotic. From Eqs. (1) and (2) one can see that $\mathbf{x}_n(i)=\mathbf{x}_n(j)\equiv\mathbf{x}_n$, $i,j=1,2,\ldots,L$, is a solution to Eq. (1), indicating that fully synchronized chaotic states are possible. For this synchronous chaotic state to be observable the corresponding N-dimensional manifold must be attracting or stable. Below we derive the criterion for the stability of this

*Electronic address: ding@walt.css.fau.edu
†Electronic address: yang@walt.css.fau.edu

synchronization manifold. Stability analysis for synchronized periodic orbits in coupled map lattices can be found in [10].

A. The case of $N=1$

We begin by considering the simplest case where the local map is one dimensional. Rewrite Eq. (1) and Eq. (2) as

$$x_{n+1}(i)=(1-\epsilon)f(x_n(i))+\frac{\epsilon}{L}\sum_{j=1}^{L} f(x_n(j)), \tag{3}$$

and

$$x_{n+1}=f(x_n). \tag{4}$$

The synchronous chaotic attractor with $x_n(i)=x_n(j)\equiv x_n$ lies along the one-dimensional diagonal in the L-dimensional phase space spanned by the vector $\mathbf{z}=[x(1),x(2),\ldots,x(L)]^T$. In other words, the synchronization manifold is the diagonal which is invariant under the dynamics. The stability of this invariant manifold can be assessed by computing its Lyapunov exponent spectrum.

Differentiating Eq. (3) and evaluating the derivatives along the synchronization trajectory leads to

$$\delta x_{n+1}(i)=(1-\epsilon)f'(x_n)\,\delta x_n(i)+\frac{\epsilon}{L}\sum_{j=1}^{L} f'(x_n)\,\delta x_n(j). \tag{5}$$

This means that the tangent vector $\delta\mathbf{z}_n=[\delta x_n(1),\delta x_n(2),\ldots,\delta x_n(L)]^T$ evolves, along the chaotic trajectory $x_n(1)=x_n(2)=\cdots=x_n(L)=x_n$ with $x_{n+1}=f(x_n)$, according to

$$\delta\mathbf{z}_{n+1}=\mathbf{J}_n\,\delta\mathbf{z}_n, \tag{6}$$

where

$$\mathbf{J}_n=f'(x_n)\begin{pmatrix} 1-(L-1)\epsilon/L & \epsilon/L & \epsilon/L & \cdots & \epsilon/L \\ \epsilon/L & 1-(L-1)\epsilon/L & \epsilon/L & \cdots & \epsilon/L \\ \vdots & \vdots & \vdots & \vdots & \vdots \\ \epsilon/L & \epsilon/L & \epsilon/L & \cdots & 1-(L-1)\epsilon/L \end{pmatrix}_{L\times L} = f'(x_n)\mathbf{J}. \tag{7}$$

Note that the constant matrix $\mathbf{J}$ is a cyclic matrix and it commutes with the following shift matrix $\mathbf{S}$:

$$\mathbf{S}=\begin{pmatrix} 0 & 1 & 0 & \cdots & 0 \\ 0 & 0 & 1 & \cdots & 0 \\ \vdots & \vdots & \vdots & \vdots & \vdots \\ 0 & 0 & 0 & \cdots & 1 \\ 1 & 0 & 0 & \cdots & 0 \end{pmatrix}_{L\times L}, \tag{8}$$

namely,

$$\mathbf{JS}=\mathbf{SJ}.$$

This implies that these two matrices share the same set of eigenvectors. The eigenvectors for $\mathbf{S}$ are known to be

$$\mathbf{E}_m=\left(\exp\left(2\pi i\frac{m-1}{L}\right),\exp\left(4\pi i\frac{m-1}{L}\right),\ldots,\exp\left(2L\pi i\frac{m-1}{L}\right)\right)^T, \tag{9}$$

where $m=1,\ldots,L$ and T denotes matrix transpose. From these eigenvectors we find that $\mathbf{J}$ has an eigenvalue of one and an $(L-1)$-fold degenerate eigenvalue of $(1-\epsilon)$.

For $m=1$ we get $\mathbf{E}_1=(1,1,\ldots,1)^T=\mathbf{v}_1$ as a real eigenvector of the constant matrix $\mathbf{J}$ in Eq. (7) pointing along the diagonal direction. The corresponding eigenvalue is one. Using $\mathbf{v}_1$ and the definition of Lyapunov exponents [11], we obtain

$$\lambda_1=\lim_{n\to\infty}\frac{1}{n}\ln\left|\left(\prod_{m=1}^{n}\mathbf{J}_m\right)\cdot\mathbf{v}_1/|\mathbf{v}_1|\right| =\lim_{n\to\infty}\frac{1}{n}\ln\left|\prod_{m=1}^{n}f'(x_m)\right|.$$

It is not surprising that the value of λ_1, describing the

stretching dynamics within the synchronization manifold, is the same as that of the one-dimensional map. In particular, from the chaos assumption earlier, $\lambda_1 > 0$.

Note that the constant matrix **J** is a symmetric matrix. This means that the eigenvectors of the eigenvalue $(1-\epsilon)$ span the $(L-1)$-dimensional subspace orthogonal to the diagonal (synchronization manifold) [12]. Choosing an arbitrary set of mutually orthonormal vectors from this subspace, $\mathbf{v}_2, \mathbf{v}_3, \ldots, \mathbf{v}_L$, we obtain the remaining $L-1$ Lyapunov exponents,

$$\lambda_2 = \lambda_3 = \cdots = \lambda_L = \lambda_1 + \ln(1-\epsilon).$$

We refer to the Lyapunov exponents $\lambda_2 = \lambda_3 = \cdots = \lambda_L$ as transversal Lyapunov exponents since they characterize the behavior of infinitesimal vectors transversal to the synchronization manifold. In other words they determine the linear stability of synchronous chaos. Note that the Lyapunov exponents found here do not depend on the lattice size L. This is in contrast to the case where the coupling is nearest neighbor (see Sec. IV).

When ϵ is relatively large such that $0 < \lambda_1 < -\ln(1-\epsilon)$, all the transversal Lyapunov exponents are negative, and the synchronous chaos state is stable and is the only observed system behavior. This result makes intuitive sense since strongly coupled systems tend to behave in unison.

As the coupling gets weaker, especially when $\lambda_1 > -\ln(1-\epsilon)$, all the transversal Lyapunov exponents become positive and the system undergoes a blowout bifurcation, through which the asynchronous state is born. For a given local one-dimensional map, the critical value of coupling is

$$\epsilon_c = 1 - e^{-\lambda_1}. \tag{10}$$

From this formula it is clear that, the more chaotic the local map, the larger the value of ϵ_c. This is again an intuitively reasonable result.

For ϵ slightly less than ϵ_c the synchronous chaos is no longer stable. However, from the assumption that the synchronization manifold is the unique attractor for $\epsilon > \epsilon_c$, we know that points far away from the synchronization manifold are still attracted to it immediately after ϵ becomes smaller than ϵ_c. This combination gives rise to the situation that, after the synchronous chaos becomes unstable, the variable that describes the distance between the system state and the synchronization manifold exhibits on-off intermittency. Below we illustrate this point with a numerical example.

Let $f(x) = 1 - ax^2$ be the logistic map. For $a = 1.9$ we have $\lambda_1 = 0.5490$. Consider a globally coupled system of $L = 100$ such maps. From Eq. (10) we get $\epsilon_c = 0.4225$. Figure 1(a) shows the dynamics for $\epsilon = 0.43 > \epsilon_c$. The variable plotted at the lattice site i is $x_n(i) - \overline{x_n}$ where the overline indicates the spatial average of the variable x. The absolute value of this quantity measures the distance between the system state and the synchronization manifold. As expected, for the 40 units displayed in the figure, we observe synchronized chaos in which the plotted quantity is uniformly zero. For $\epsilon = 0.41$, which is slightly below ϵ_c, clearly identified episodes of synchronized behavior are seen in Fig. 1(b) which is interspersed with bursts away from the synchronization attractor, suggesting the occurrence of on-off intermittency. This intermittent dynamics is eventually replaced by fully developed asynchronous chaos as the parameter $\epsilon = 0.385$ is far removed from the critical value, as shown in Fig. 1(c).

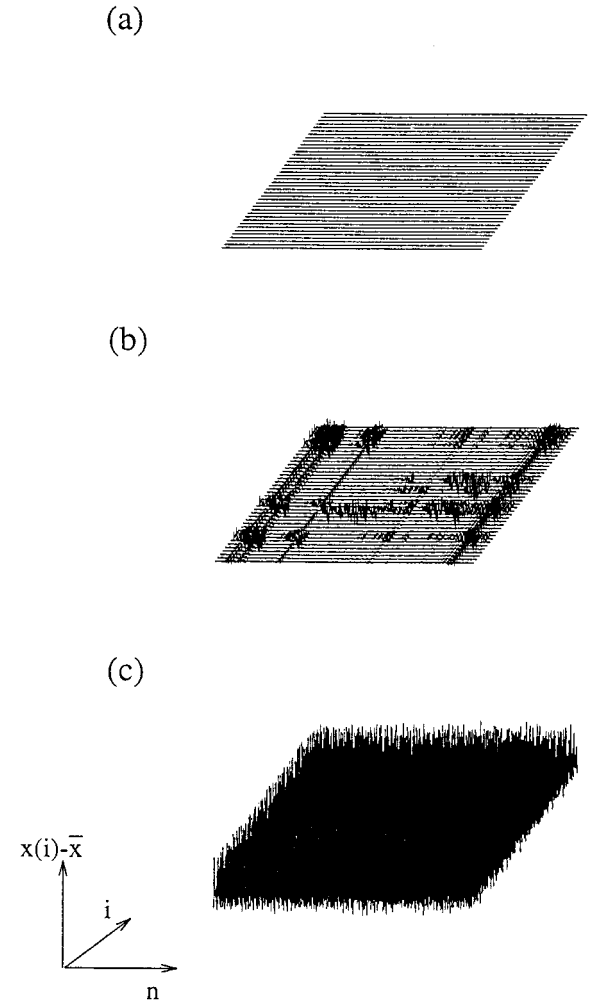

FIG. 1. The time series, $x(i) - \overline{x}$, from 40 of 100 globally coupled logistic maps. The overbar indicates spatial average. (a) $\epsilon = 0.43 > \epsilon_c = 0.4225$, (b) $\epsilon = 0.41$, which is slightly less than ϵ_c, and (c) $\epsilon = 0.385$, which is further away from the critical value ϵ_c.

B. The case of $N > 1$

Now let us assume that the local map **f** in Eq. (1) is $N > 1$ dimensional. This local N-dimensional map

$$\mathbf{x}_{n+1} = \mathbf{f}(\mathbf{x}_n) \tag{11}$$

admits N Lyapunov exponents denoted by $h_1 \geqslant h_2 \geqslant \cdots \geqslant h_N$. Here **x** is an N-dimensional column vector. Let

$$\mathbf{A}_n = \mathbf{D}_{\mathbf{x}}\mathbf{f}(\mathbf{x}_n) \tag{12}$$

be the Jacobian matrix of the local map. From the theory of Lyapunov exponents [11], for a typical initial condition $\mathbf{x}_1$ in the proper basin of attraction, we can find a set of N unit vectors $\mathbf{e}_1, \mathbf{e}_2, \ldots, \mathbf{e}_N$ such that

$$h_i = \lim_{n\to\infty} \frac{1}{n} \ln \left| \left(\prod_{m=1}^{n} \mathbf{A}_m \right) \cdot \mathbf{e}_i \right|. \tag{13}$$

Note that, if we pick an N-dimensional unit vector $\mathbf{e}$ at random, then a calculation similar to that in the above formula will always yield the largest Lyapunov exponent h_1.

Consider the coupled system Eq. (1). The phase space now is $L\times N$ dimensional. Let us form the phase space vector as

$$\mathbf{z}=[\mathbf{x}^T(1),\mathbf{x}^T(2),\ldots,\mathbf{x}^T(L)]^T.$$

In other words, $\mathbf{z}$ is an $(L\times N)$-dimensional column vector. The synchronization manifold, defined by $\mathbf{x}_n(i)=\mathbf{x}_n(j)$, $i,j=1,2,\ldots,L$, is N dimensional and the dynamics in the manifold evolves according to Eq. (11).

Consider an infinitesimal deviation from this manifold $\delta\mathbf{z}_n$. Then, from Eq. (1) and along a synchronization trajectory, we have

$$\delta\mathbf{z}_{n+1}=\mathbf{J}_n\delta\mathbf{z}_n, \tag{14}$$

where

$$\mathbf{J}_n=\begin{pmatrix} [1-(L-1)\epsilon/L]\mathbf{A}_n & (\epsilon/L)\mathbf{A}_n & (\epsilon/L)\mathbf{A}_n & \cdots & (\epsilon/L)\mathbf{A}_n \\ (\epsilon/L)\mathbf{A}_n & [1-(L-1)\epsilon/L]\mathbf{A}_n & (\epsilon/L)\mathbf{A}_n & \cdots & (\epsilon/L)\mathbf{A}_n \\ \vdots & \vdots & \vdots & \vdots & \vdots \\ (\epsilon/L)\mathbf{A}_n & (\epsilon/L)\mathbf{A}_n & (\epsilon/L)\mathbf{A}_n & \cdots & [1-(L-1)\epsilon/L]\mathbf{A}_n \end{pmatrix} \tag{15}$$

is an $(L\times N)\times(L\times N)$ matrix.

The spectrum of all the Lyapunov exponents with respect to the synchronization solution can be evaluated in a fashion similar to that of one dimensional local maps. Considering vectors of the form

$$\mathbf{v}_i^{\text{parallel}}=[\mathbf{e}_i^T,\mathbf{e}_i^T,\ldots,\mathbf{e}_i^T]^T,$$

where $\mathbf{e}_i$ is the same vector as that used in Eq. (13), we obtain the Lyapunov exponents describing the dynamics within the synchronization manifold through

$$\lambda_i^{\text{parallel}}=\lim_{n\to\infty}\frac{1}{n}\ln\left|\left(\prod_{m=1}^{n}\mathbf{J}_m\right)\cdot\mathbf{v}_i^{\text{parallel}}\Big/\,|\mathbf{v}_i^{\text{parallel}}|\right| \tag{16}$$

$$=\lim_{n\to\infty}\frac{1}{n}\ln\left|\left(\prod_{m=1}^{n}\mathbf{A}_m\right)\cdot\mathbf{e}_i\right|, \tag{17}$$

which, as expected, is h_i.

To describe the dynamics transversal to the synchronization manifold let us form vectors as

$$\mathbf{v}_i^{\text{vertical}}=[a_1\mathbf{e}_i^T,a_2\mathbf{e}_i^T,\ldots,a_L\mathbf{e}_i^T]^T,$$

where a_i's are chosen such that $[a_1,a_2,\ldots,a_L]$ is an L-dimensional unit vector orthogonal to the vector $[1,1,\ldots,1]$. Note that such vectors are eigenvectors of the constant matrix $\mathbf{J}$ in Eq. (7) with eigenvalue $(1-\epsilon)$. A calculation similar to that in Eq. (17) gives the distinct set of all transversal Lyapunov exponents,

$$\lambda_i^{\text{vertical}}=h_i+\ln(1-\epsilon).$$

So the largest transversal Lyapunov exponent is

$$\lambda_1^{\text{vertical}}=h_1+\ln(1-\epsilon).$$

From this we calculate the critical value of coupling ϵ_c to be

$$\epsilon_c=1-e^{-h_1}. \tag{18}$$

Note the similarity between Eq. (10) and Eq. (18). As a result we conclude that, for $\epsilon<\epsilon_c$, the synchronous chaotic state is no longer stable and we observe the onset of on-off intermittency.

We now illustrate the above theoretical criterion for the bifurcation of synchronous chaos with an example where the local map is the $(N=2)$-dimensional Hénon map,

$$x_{n+1}=y_n+1-ax_n^2, \tag{19}$$

$$y_{n+1}=bx_n. \tag{20}$$

For $a=1.4$ and $b=0.3$ the largest Lyapunov exponent is calculated to be $h_1=0.4207$. Consider a globally coupled system of $L=100$ such maps. From Eq. (18) we get $\epsilon_c=0.3434$. The variable of interest here is the distance between the system state and the synchronization manifold measured by

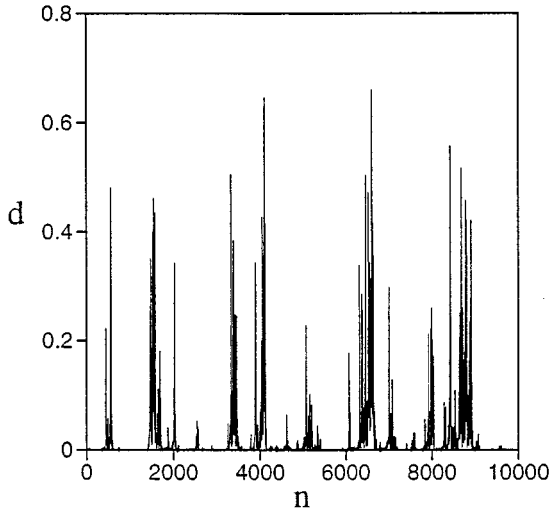

FIG. 2. The value of $d=(1/L)\,\Sigma_{i=1}^{L}|x(i)-\overline{x}|$ as a function of time n from $L=100$ globally coupled Hénon maps. Here $\epsilon=0.34$ is slightly less than $\epsilon_c=0.3434$.

$$d_n=\frac{1}{L}\sum_{i=1}^{L}|x_n(i)-\overline{x_n}|.$$

Here the overbar denotes the spatial average of the variable inside. For $\epsilon>\epsilon_c$, the value of d_n is uniformly zero in the long run for any initial condition, indicating the presence of synchronized chaotic attractor. Figure 2 shows the on-off intermittent time series for $\epsilon=0.338$ which is slightly less than ϵ_c.

III. CHARACTERISTICS OF ON-OFF INTERMITTENT TIME SERIES

The characterization of on-off intermittent time series like the one shown in Fig. 2 has been extensively studied in the past [3–7]. We will not duplicate these analyses here. Instead our goal is to point out the mathematical origin that enables the past analyses and results to be applicable to the present spatiotemporal on-off intermittency problem.

A. Theoretical considerations

The on-off intermittent time series, for parameter values close to the critical point, spends most of the time in the off state, suggesting that the system state is near the synchronization manifold. The time series in this case show universal properties.

To see the reason, consider the case where the local map is one dimensional ($L=1$). Let d_n denote the absolute value of the projection of $\delta\mathbf{z}_n$ of Eq. (6) onto any unit vector $\mathbf{v}$ that is perpendicular to the diagonal, $d_n=|\mathbf{v}^T\mathbf{z}_n|$. The value of d_n can be viewed as measuring the distance between the trajectory and the synchronization manifold and evolves according to

$$d_{n+1}=|(1-\epsilon)f'(x_n)|d_n=\eta_n d_n, \tag{21}$$

where $\eta_n=|(1-\epsilon)f'(x_n)|$.

Clearly, $d=0$ is a fixed point for Eq. (21), reflecting the fact that the synchronization manifold is invariant. According to [6,7] this $d=0$ fixed point is stable if $\langle\ln|z_n|\rangle$ is negative where $\langle\ \rangle$ denotes temporal average. This is equivalent to saying that $\lambda_1+\ln(1-\epsilon)<0$, the same stability condition derived earlier using Lyapunov exponents. As past work has shown, it is the linear equation with parametric driving in Eq. (21) that underlies the observed universal characters of the on-off intermittent time series. This is why we should expect the same characteristics for on-off intermittent time series found in earlier works to be applicable to the present problem.

The case where the local map is $N>1$ dimensional is not as simple. To see what to expect here, we again examine the projection of $\delta\mathbf{z}_n$ in Eq. (14) onto a unit vector of the form

$$\mathbf{v}=[a_1\mathbf{e}^T,a_2\mathbf{e}^T,\ldots,a_L\mathbf{e}^T]^T,$$

where $\mathbf{e}$ is an N-dimensional unit vector picked at random and $[a_1,a_2,\ldots,a_L]^T$ is an L-dimensional unit vector orthogonal to the diagonal. This vector $\mathbf{v}$ is orthogonal to the N-dimensional synchronization manifold. Letting d_n denote the absolute value of the projection, from Eqs. (14) and (15), we get

$$d_{n+1}=|(1-\epsilon)y_n|\hat{d}_n=\eta_n\hat{d}_n, \tag{22}$$

where $\hat{d}_n=\hat{\mathbf{v}}^T\delta\mathbf{z}_n$, $\hat{\mathbf{v}}=[a_1\hat{\mathbf{e}}^T,a_2\hat{\mathbf{e}}^T,\ldots,a_L\hat{\mathbf{e}}^T]^T$, and $y_n\hat{\mathbf{e}}^T=\mathbf{e}^T\mathbf{A}_n$. Note that $\hat{\mathbf{e}}$ is still a unit vector and y_n is a multiplicative scalar that describes the amount of stretching due to the application of $\mathbf{A}_n$. Although d_{n+1} and $\hat{d}_n$ represent projections of the tangent vectors $\delta\mathbf{z}_{n+1}$ and $\delta\mathbf{z}_n$ onto two different directions, both directions are orthogonal to the synchronization manifold. Thus we can still think of them as measures of the distance between the trajectory point and the synchronization manifold. In this sense Eq. (22) and Eq. (21) play a similar role and we may expect the on-off intermittent time series from coupled ($N>1$)-dimensional maps to share the same universal properties as that from coupled one-dimensional maps.

B. Numerical results

We illustrate the properties of on-off intermittent time series with three quantities: laminar phase distributions, power spectra, and mean bursting amplitude as a function of the coupling strength ϵ.

Suppose d is the variable plotted against time. Let τ denote the threshold value of d such that for $d>\tau$ the signal is considered on and for $d<\tau$ the signal is considered off. The length of the laminar phase, denoted by T, is defined as the length of the off state. In practice one should choose τ in such a way that when $d<\tau$ the linear approximation in Eq. (21) or Eq. (22) is valid.

For a typical chaotic local map, analysis in [7,13] (see also [6]), which is based on a model like Eq. (21) and a random walk analogy, shows that the distribution of the laminar phase T is in the form

$$P(T)\sim T^{-3/2}e^{-T/T_s}, \tag{23}$$

where

$$T_s\sim(\epsilon_c-\epsilon)^{-2} \tag{24}$$

gives the crossover point from a power law behavior with an exponent $-3/2$ to an exponential behavior.

In Fig. 3(a) we plot the numerically calculated histogram for the length of the laminar phase for 100 globally coupled logistic maps. The on-off intermittent time series used here is constructed in the same way as that shown in Fig. 2. We choose $\tau=0.01$ and collect 1 000 000 distinct laminar phases for statistics. Two values of ϵ are considered: $\epsilon_1=0.415$ (plus) and $\epsilon_2=0.4075$ (triangle). Recall that $\epsilon_c=0.4225$ in this case. The straight line in the figure has a slope of $-3/2$ and is plotted to guide the eye only. From the figure we can see that the numerical results conform to the theoretical prediction in Eq. (23). In particular, the crossover from power law to exponential occurs earlier as ϵ is moved further away from ϵ_c. The quantitative prediction concerning this behavior is contained in Eq. (24) and is confirmed for the coupled logistic maps in Fig. 4 where T_s is obtained and plotted for a number of ϵ values.

Figure 3(b) shows the numerically calculated histogram for the on-off intermittent time series in Fig. 2 for 100 globally coupled Hénon maps. We use $\tau=0.01$ and the same set of parameters as that used for Fig. 2. Again a straight line of

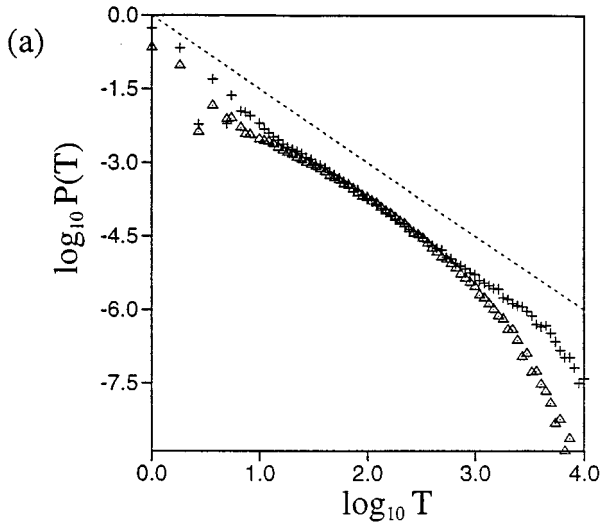

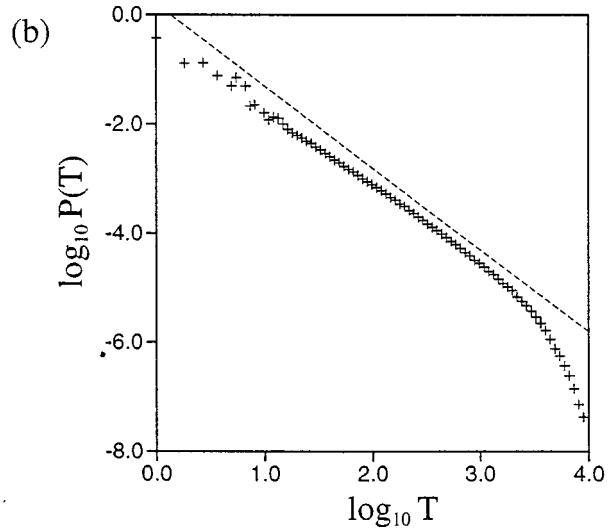

FIG. 3. (a) Log-log plot of the histogram for the laminar phase interval distribution for the on-off intermittent time series from 100 coupled logistic maps. The time series used here is constructed in the same way as that used in Fig. 2. (b) Log-log plot of the histogram for the laminar phase interval distribution for the on-off time series shown in Fig. 2.

slope $-3/2$ is drawn in the figure to guide the eye. Clearly, the same power law and exponential crossover behavior is observed here for coupled $(N>1)$-dimensional maps.

Figure 5 shows the power spectrum for the globally coupled logistic maps with $a=1.9$ and $\epsilon=0.41$. The two straight lines in the figure have slopes of $-1/2$ and -2, respectively. It is predicted in [4] that one should observe three distinct regions of scaling behavior in the power spectrum of on-off intermittent time series. For small frequencies the spectral density should be a constant. For intermediate frequencies the spectral density $S(f)$ scales with frequency f as

$$S(f)\sim(1/f)^{1/2}.$$

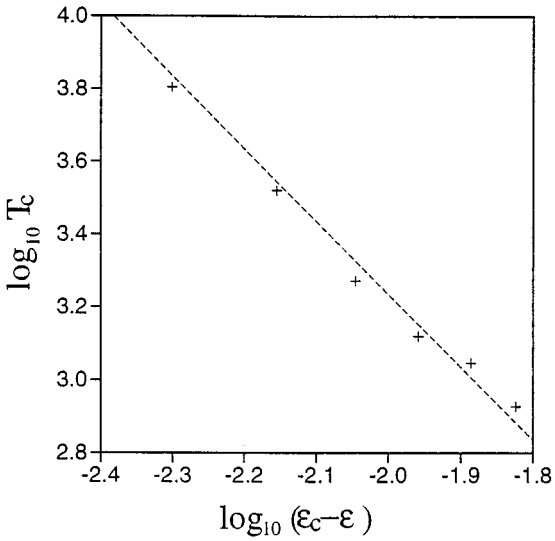

FIG. 4. Log-log plot of the crossover time T_s [see Eqs. (23) and (24)] as a function of the parameter $\epsilon_c-\epsilon$.

For large frequencies $S(f)$ should scale with f as

$$S(f)\sim(1/f)^2.$$

In Fig. 5 we see the predicted behavior for the intermediate and large frequency regions clearly. However, the predicted low frequency behavior is not observed. This could be due to the prohibitively long time series required for the appearance of such behavior.

Our last numerical result is shown in Fig. 6. Here we consider the globally coupled logistic maps with $a=1.9$ and plot the mean bursting amplitude as a function of the parameter $\epsilon_c-\epsilon$. Theory in [5] predicts a linear relationship between the two quantities. This is clearly the case from the figure.

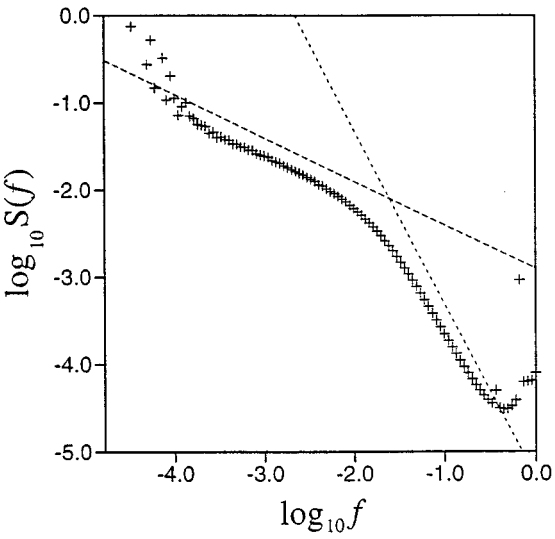

FIG. 5. Log-log plot of the power spectrum for on-off intermittent time series from 100 globally coupled logistic maps.

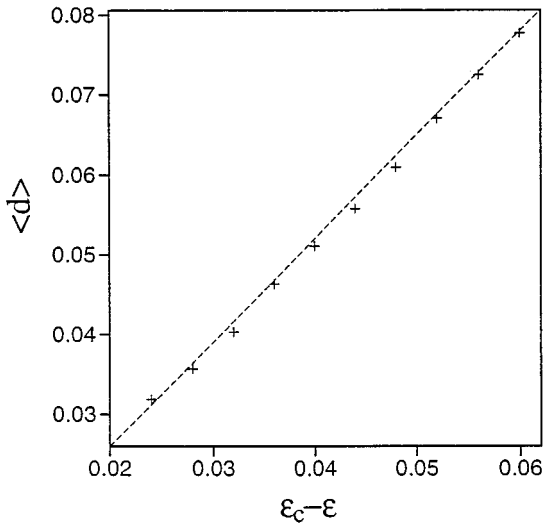

FIG. 6. Average bursting amplitude for on-off intermittent time series from 100 globally coupled logistic maps as a function of the parameter $\epsilon_c-\epsilon$.

IV. NEAREST-NEIGHBOR COUPLING AND THE STABILITY OF SYNCHRONOUS CHAOS

Consider the following coupled map lattice model where the coupling is nearest neighbor:

$$x_{n+1}(i)=(1-\epsilon)f(x_n(i))+\frac{\epsilon}{2}[f(x_n(i-1))+f(x_n(i+1))]. \tag{25}$$

Here we assume one-dimensional local maps and impose the periodic boundary condition $x_n(0)=x_n(L)$. Similar discussions can be carried out for the case of $(N>1)$-dimensional local maps.

Like the case of global coupling, from Eq. (25), we see that the synchronous chaotic state is invariant under the dynamics. We proceed to compute the Lyapunov spectrum for the synchronization attractor.

The Jacobian matrix for Eq. (25) at time n calculated along the synchronous chaotic trajectory $x_n(i)=x_n(j)=x_n$ with $x_{n+1}=f(x_n)$ is the following $L\times L$ matrix:

$$\mathbf{K}_n=f'(x_n)\begin{pmatrix}(1-\epsilon) & \epsilon/2 & 0 & \cdots & 0 & \epsilon/2\\ \epsilon/2 & (1-\epsilon) & \epsilon/2 & \cdots & 0 & 0\\ \vdots & \vdots & \vdots & \vdots & \vdots & \vdots\\ 0 & 0 & 0 & \cdots & (1-\epsilon) & \epsilon/2\\ \epsilon/2 & 0 & 0 & \cdots & \epsilon/2 & (1-\epsilon)\end{pmatrix}=f'(x_n)\mathbf{K}.$$

The matrix $\mathbf{K}$ is also a cyclic matrix and commutes with the matrix $\mathbf{S}$ in Eq. (8), i.e., $\mathbf{KS}=\mathbf{SK}$. Hence the eigenvectors for the Jacobian matrix $\mathbf{K}$ are still in the form of Eq. (9), namely,

$$\mathbf{E}_m=\left(\exp\left(2\pi i\frac{m-1}{L}\right),\exp\left(4\pi i\frac{m-1}{L}\right),\ldots,\exp\left(2L\pi i\frac{m-1}{L}\right)\right)^T, \tag{26}$$

where $m=1,\ldots,L$ and T represents matrix transpose.

From these eigenvectors and the definition of Lyapunov exponents [11] we obtain the Lyapunov exponent spectrum for Eq. (25) as

$$\lambda_1=\lim_{n\to\infty}\frac{1}{n}\ln\left|\prod_{m=1}^{n}f'(X_m(i))\right|,$$

$$\lambda_2=\lambda_1+\ln[1-\epsilon+\epsilon\cos(2\pi/L)],$$

$$\vdots$$

$$\lambda_L=\begin{cases}\lambda_1+\ln(1-2\epsilon) & \text{if } L \text{ even}\\ \lambda_1+\ln[1-\epsilon-\epsilon\cos(2\pi/L)] & \text{if } L \text{ odd}\end{cases}$$

ordered in a descending fashion.

Unlike the Lyapunov exponents in globally coupled systems, the Lyapunov exponents in the present system are functions of the system size L. In particular, for large L, the largest transversal Lyapunov exponent λ_2 is nearly the same as λ_1 which by definition is positive. This, coupled with the natural limitation that $\epsilon\leqslant 1$, means that a large nearest-neighbor coupled system does not have a stable synchronous chaotic attractor. For a given individual map, i.e., λ_1 is fixed, let us calculate the maximum lattice size L_m under which we can still observe synchronous chaos. Clearly, the larger the coupling strength, the larger the size L_m. By letting $\epsilon=1$ and $\lambda_2=0$ we have,

$$L_m=\mathrm{int}\left(\frac{2\pi}{\cos^{-1}[\exp(-\lambda_1)]}\right), \tag{27}$$

where the function int( ) gives the largest integer that is equal to or less than the argument.

To get a concrete idea of the value of L_m, suppose that the local map is the surjective logistic map, $f(x)=1-2x^2$. We know that $\lambda_1=\ln 2$ in this case. From Eq. (27) we get

$L_m = 6$. That is, for a system with more than six nearest-neighbor coupled surjective logistic maps, one can no longer observe stable synchronous chaos.

V. CONCLUSIONS

The main results of this paper are as follows.

(1) For globally coupled map lattices, we derive explicit conditions for calculating the parameter value at which the synchronous chaotic state becomes unstable and bifurcates into an asynchronous chaotic state.

(2) We show that the on-off intermittent time series, immediately after the synchronous chaotic state becomes unstable, has universal characteristics.

(3) For nearest-neighbor coupled systems, we show that the stability of the synchronous chaotic attractor is a function of the system size. In particular, we can only expect to observe synchronous chaos in such systems if the number of coupled maps is small.

[1] See, for example, K. Kaneko, CHAOS **2**, 279 (1992), and other articles in this special focus issue on coupled map lattices.

[2] E. Ott and J. C. Sommerer, Phys. Lett. A **188**, 39 (1994).

[3] A. S. Pikovsky, Z. Phys. B **55**, 149 (1984); H. Fujisaka and T. Yamada, Prog. Theor. Phys. **74**, 918 (1985); N. Platt, E. A. Spiegel, and C. Tresser, Phys. Rev. Lett. **70**, 279 (1993); N. Platt, S. M. Hammel, and J. F. Heagy, *ibid.* **72**, 3498 (1994); P. W. Hammer *et al.*, *ibid.* **73**, 1095 (1994).

[4] H. Fujisaka, H. Ishi, M. Inoue, and T. Yamada, Prog. Theor. Phys. **76**, 1198 (1986).

[5] L. Yu, E. Ott, and Q. Chen, Phys. Rev. Lett. **65**, 2935 (1990); Physica D **53**, 102 (1991).

[6] J. F. Heagy, N. Platt, and S. M. Hammel, Phys. Rev. E **49**, 1140 (1994).

[7] M. Ding and W. Yang, Phys. Rev. E **52**, 207 (1995).

[8] For a sample of papers on riddled basins see E. Ott, J. C. Sommerer, J. C. Alexander, I. Kan, and J. A. Yorke, Phys. Rev. Lett. **71**, 4134 (1993); J. C. Sommerer and E. Ott, Nature (London) **365**, 136 (1993); P. Ashwin, J. Buescu, and I. N. Stewart, Phys. Lett. A **193**, 126 (1993); E. Ott, J. C. Alexander, I. Kan, J. C. Sommerer, and J. A. Yorke, Physica D **76**, 384 (1994); Y. C. Lai and R. L. Winslow, Phys. Rev. Lett. **72**, 1640 (1994); R. H. Parmenter and L. Y. Yu, Phys. Lett. A **189**, 181 (1994); J. F. Heagy, T. L. Carroll, and L. M. Pecora, Phys. Rev. Lett. **73**, 3528 (1994); T. Kapitaniak, J. Phys. A **28**, L63 (1995); M. Ding and W. Yang, Phys. Rev. E **54**, 2489 (1996).

[9] M. Ding and L. T. Wille, Phys. Rev. E **48**, 1605 (1993); W. Yang, E. J. Ding, and M. Ding, Phys. Rev. Lett. **76**, 1808 (1996).

[10] R. E. Amritkar, P. M. Gade, A. D. Gangal, and V. M. Nandkumaran, Phys. Rev. A **44**, R3407 (1991).

[11] E. Ott, *Chaos in Dynamical Systems* (Cambridge University Press, Cambridge, Great Britain, 1993); J.-P. Eckmann and D. Ruelle, Rev. Mod. Phys. **57**, 617 (1985).

[12] For example, the imaginary parts of the vectors in Eq. (9) for $m = 2,3,\ldots,L$ can be the vectors to span such a subspace.

[13] For typical chaotic maps, the autocorrelation function for the variable η_n in Eq. (21) decays exponentially. This means that we should use the ordinary Brownian motion exponent $H = 1/2$ when applying the theory in [7].